IL-9–mediated survival of type 2 innate lymphoid cells promotes damage control in helminth-induced lung inflammation

Jan-Eric Turner,[1,2] Peter J. Morrison,[1] Christoph Wilhelm,[1,3] Mark Wilson,[1] Helena Ahlfors,[1] Jean-Christophe Renauld,[4] Ulf Panzer,[2] Helena Helmby,[5] and Brigitta Stockinger[1]

[1]Division of Molecular Immunology, Medical Research Council National Institute for Medical Research, London NW7 1AA, England, UK
[2]III. Medizinische Klinik und Poliklinik, Universitätsklinikum Hamburg-Eppendorf, 20246 Hamburg, Germany
[3]Mucosal Immunology Section, Laboratory of Parasitic Diseases, National Institute of Allergy and Infectious Diseases, National Institutes of Health, Bethesda, MD 20892
[4]de Duve Institute, Catholic University of Louvain and Ludwig Institute for Cancer Research, Brussels Branch, B-1200 Brussels, Belgium
[5]London School of Hygiene and Tropical Medicine, London WC1E 7HT, England, UK

IL-9 fate reporter mice established type 2 innate lymphoid cells (ILC2s) as major producers of this cytokine in vivo. Here we focus on the role of IL-9 and ILC2s during the lung stage of infection with *Nippostrongylus brasiliensis*, which results in substantial tissue damage. IL-9 receptor (IL-9R)–deficient mice displayed reduced numbers of ILC2s in the lung after infection, resulting in impaired IL-5, IL-13, and amphiregulin levels, despite undiminished numbers of Th2 cells. As a consequence, the restoration of tissue integrity and lung function was strongly impaired in the absence of IL-9 signaling. ILC2s, in contrast to Th2 cells, expressed high levels of the IL-9R, and IL-9 signaling was crucial for the survival of activated ILC2s in vitro. Furthermore, ILC2s in the lungs of infected mice required the IL-9R to up-regulate the antiapoptotic protein BCL-3 in vivo. This highlights a unique role for IL-9 as an autocrine amplifier of ILC2 function, promoting tissue repair in the recovery phase after helminth-induced lung inflammation.

CORRESPONDENCE
Brigitta Stockinger:
bstocki@nimr.mrc.ac.uk

Abbreviations used: 7AAD, 7-amino-actinomycin D; EdU, 5′-ethynyl-2′-deoxyuridine; eYFP, enhanced YFP; ILC, innate lymphoid cell; MDLN, mediastinal LN.

The cytokine IL-9 was discovered more than 20 yr ago and described as a T cell and mast cell growth factor produced by T cell clones (Uyttenhove et al., 1988; Hültner et al., 1989; Schmitt et al., 1989). Subsequently, IL-9 was shown to promote the survival of a variety of different cell types in addition to T cells (Hültner et al., 1990; Gounni et al., 2000; Fontaine et al., 2008; Elyaman et al., 2009). Until recently, Th2 cells were thought to be the dominant source of IL-9 and the function of IL-9 was mainly studied in the context of Th2 type responses in airway inflammation and helminth infections (Godfraind et al., 1998; Townsend et al., 2000; McMillan et al., 2002; Temann et al., 2002). IL-9 blocking antibodies were shown to ameliorate lung inflammation (Cheng et al., 2002; Kearley et al., 2011) and are currently in clinical trials for the treatment of patients with asthma (Parker et al., 2011). The paradigm that Th2 cells are the dominant source of IL-9 was challenged when it became apparent that naive $CD4^+$ T cells cultured in the presence of TGF-β and IL-4 initiate high IL-9 expression without coexpression of IL-4, suggesting the existence of a dedicated subset of IL-9–producing T cells (Dardalhon et al., 2008; Veldhoen et al., 2008; Angkasekwinai et al., 2010; Chang et al., 2010; Staudt et al., 2010). Subsequently, the generation of an IL-9–specific reporter mouse strain enabled the study of IL-9–producing cell types in vivo and revealed that in a model of lung inflammation IL-9 is produced by innate lymphoid cells (ILCs) and not T cells (Wilhelm et al., 2011). IL-9 production in ILCs was transient

J.-E. Turner and P.J. Morrison contributed equally to this paper.

The Rockefeller University Press $30.00
J. Exp. Med. 2013 Vol. 210 No. 13 2951-2965
www.jem.org/cgi/doi/10.1084/jem.20130071

The Journal of Experimental Medicine

but important for the maintenance of IL-5 and IL-13 in ILCs. Such type 2 cytokine-producing ILCs (ILC2s; Spits and Di Santo, 2011) were first described as a population of IL-5– and IL-13–producing non-B/non-T cells (Fort et al., 2001; Hurst et al., 2002; Fallon et al., 2006; Voehringer et al., 2006) and later shown to play a role in helminth infection via IL-13 expression (Moro et al., 2010; Neill et al., 2010; Price et al., 2010; Saenz et al., 2010). In addition, important functions were ascribed to such cells in the context of influenza infection (Chang et al., 2011; Monticelli et al., 2011) and airway hyperactivity in mice (Barlow et al., 2012) and humans (Mjösberg et al., 2011). However, although the contribution of ILC2s to host immunity against helminths in the gut is well established (Moro et al., 2010; Neill et al., 2010; Price et al., 2010; Saenz et al., 2010), the function of ILC2s in helminth-related immune responses in the lung remains unknown. ILC2s are marked by expression of the IL-33R (Moro et al., 2010; Neill et al., 2010; Price et al., 2010), as well as the common γ chain (γ_c) cytokine receptors for IL-2 and IL-7 (Moro et al., 2010; Neill et al., 2010). Interestingly, gene expression array analyses have demonstrated that the receptor for IL-9, another member of the γ_c receptor family, is also expressed in ILC2s and differentiates them from Th2 cells (Price et al., 2010) and ROR-γt$^+$ ILCs (Hoyler et al., 2012). However, the function of IL-9R expression for ILC2 biology has not been addressed so far.

Here we show that the production of IL-5, IL-13, and amphiregulin during infection with *Nippostrongylus brasiliensis* in the lung depends on ILC2s and their expression of IL-9R. The ability to signal via the IL-9R was crucial for the survival of ILC2s, but not Th2 cells. The absence of IL-9 signaling in IL-9R–deficient mice resulted in reduced lung ILC2 numbers and, consequently, diminished repair of lung damage in the chronic phase after helminth-induced lung injury despite the presence of an intact Th2 cell response. Thus, we identify IL-9 as a crucial autocrine amplifier of ILC2 function and survival.

RESULTS

IL-9 expression in the lung during *N. brasiliensis* infection

The larval stage of *N. brasiliensis* travels from the skin to the lung, where it exerts substantial tissue damage before reaching the gut where a protective immune response leads to worm expulsion in immunocompetent mice (Camberis et al., 2003; Harvie et al., 2010). Although IL-9–deficient mice on a mixed background display unimpaired *N. brasiliensis* expulsion, an involvement of IL-9 in helminth-induced lung inflammation was not addressed (Townsend et al., 2000). To visualize IL-9 expression, we bred *IL9^{Cre}* mice with reporter mice, expressing enhanced YFP (eYFP) under the control of the endogenous Rosa 26 promoter (termed *R26R^{eYFP}*). In this mouse strain, termed *IL9^{Cre}R26R^{eYFP}*, the fluorescent reporter will permanently label cells that had expressed the IL-9 gene irrespective of the current production of this cytokine (Wilhelm et al., 2011). To address the kinetics of IL-9 expression in the lungs, we infected *IL9^{Cre}R26R^{eYFP}* reporter mice with L3 stage larvae of *N. brasiliensis* by subcutaneous injection. IL-9 expression, as monitored by eYFP expression, was dominant in the late stage after *N. brasiliensis* infection at a time the helminth larvae had left the lung and were expelled from the gut (day 12; Fig. 1 A; Harvie et al., 2010). IL-9–expressing cells, which were exclusively Thy1.2$^+$, could be recovered from the lung tissue but were very rare in the draining LNs (Fig. 1, A–C). Although protein expression of IL-9 was maximal around day 9 and had waned after 12 d (Fig. 1 D), cells that had once expressed IL-9 were still detectable in the lung at day 20 after the infection (Fig. 1, A and B). Throughout the time course of the infection, the vast majority of the Thy1.2$^+$ IL-9–expressing cells were lineage-negative, non-T cells, thus pinpointing ILCs as the major source of IL-9 (Fig. 1, E–G). To address the question of whether IL-9–expressing T cells, although low in numbers as compared with the IL-9–expressing ILCs, might contribute significantly to total IL-9 production in the lung of *N. brasiliensis*–infected mice, we compared *Il9* mRNA expression in eYFP$^+$ T cells and eYFP$^+$ ILCs sorted from the same *IL9^{Cre}R26R^{eYFP}* reporter mice at day 12 of the infection (Fig. 1 H). In these paired samples, eYFP$^+$ ILCs showed higher levels of *Il9* mRNA transcripts than eYFP$^+$ T cells, suggesting that IL-9–expressing ILCs not only outnumber IL-9–expressing T cells, but also express more IL-9 on a cellular level.

Further analysis confirmed that eYFP$^+$Thy1.2$^+$Lin$^-$ cells were marked by the surface expression of CD25, IL-7Rα (CD127), IL-33R (T1/ST2), ICOS (inducible T cell costimulator), c-Kit (tyrosine protein kinase kit), Sca-1 (stem cell antigen-1) and the production of high amounts of IL-13 and IL-5, but little IL-4, IL-17A, or IFN-γ (not depicted). Furthermore, eYFP$^+$Thy1.2$^+$Lin$^-$ cells sorted from the lungs of infected mice expressed high levels of the ILC2-related transcription factors *Rora* (*retinoid acid receptor–related orphan receptor α*; Wong et al., 2012) and *Gata3* (Hoyler et al., 2012; Liang et al., 2012) but showed no expression of *Rorc* (not depicted), a transcription factor of IL-17A– and IL-22–producing ILCs (Spits and Di Santo, 2011). Thus, ILC2s represent the dominant IL-9–producing cell type in the lung during infection with *N. brasiliensis*.

ILC2 accumulation in the lung tissue depends on IL-9R signaling

High expression of the IL-9R on ILC2s residing in the gut-associated lymphoid tissue has been described previously (Price et al., 2010; Hoyler et al., 2012). To address whether lung ILCs have the propensity to respond to IL-9, we assessed IL-9R expression of the total Thy1.2$^+$Lin$^-$ ILC population in the lung. Indeed, ILCs from naive and *N. brasiliensis*–infected mice displayed high levels of *Il9r* mRNA expression, much higher than CD4$^+$ T cells isolated from the same animals (Fig. 2 A).

To investigate the functional role of the IL-9R in the context of helminth-induced lung injury, we infected C57BL/6 WT and C57BL/6 IL-9R–deficient (*Il9r$^{-/-}$*) mice with *N. brasiliensis*. As previously described (Price et al., 2010), we

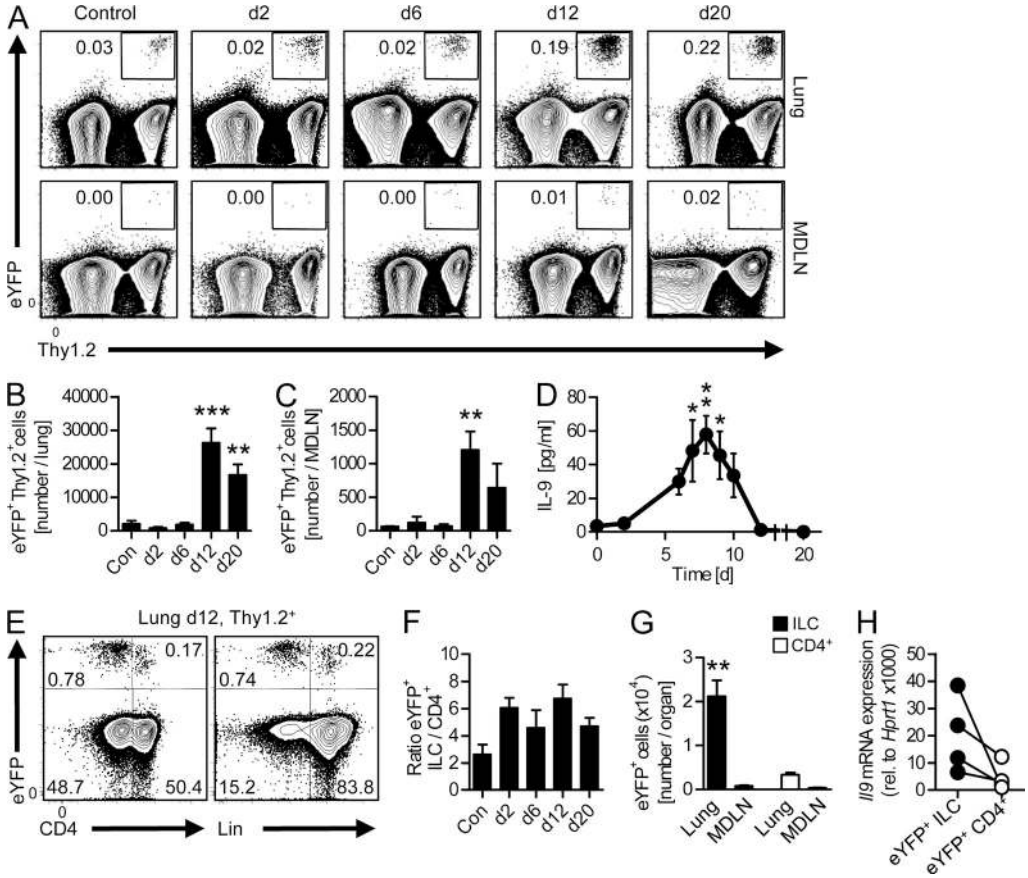

Figure 1. IL-9 expression in the lung during *N. brasiliensis* infection. (A) Flow cytometry of lung and MDLN cells from *IL9*^{Cre}*R26R*^{eYFP} mice at days 2, 6, 12, and 20 after *N. brasiliensis* infection as well as from naive *Il9*^{Cre}*R26R*^{eYFP} controls. Plots are gated for CD45$^+$ lymphoid cells. Numbers represent percentage of eYFP$^+$Thy1.2$^+$ cells of total cells gated. (B and C) Absolute numbers of eYFP$^+$Thy1.2$^+$ cells in lungs (B) and MDLNs (C) at the respective time points (n = 3–4 per time point; **, P < 0.01; ***, P < 0.001). (D) IL-9 protein concentration in the lungs of *N. brasiliensis*–infected WT mice and in naive controls (day 0; $n \geq 4$ per time point; *, P < 0.05; **, P < 0.01). (E) Flow cytometry of lung cells from *IL9*^{Cre}*R26R*^{eYFP} mice stained for CD45, Thy1.2, CD4, and lineage markers (Lin, including CD3, CD4, CD8, CD11b, CD11c, CD19, CD49b, TCR-β, TCR-γ, NK1.1, GR-1, and Ter119) at day 12 after *N. brasiliensis* infection. Plots are gated for CD45$^+$Thy1.2$^+$ lymphoid cells, and numbers indicate the percentage of cells in each quadrant. (F) Ratio of eYFP$^+$ ILCs and eYFP$^+$CD4$^+$ T cells at various time points after the infection (n = 3–4 per time point). (G) Absolute number of eYFP$^+$ ILCs and eYFP$^+$CD4$^+$ T cells in lungs and MDLNs of *IL9*^{Cre}*R26R*^{eYFP} mice at day 12 after *N. brasiliensis* infection (n = 4 per group; **, P = 0.003 vs. lung CD4). (H) Quantitative RT-PCR analysis of *Il9* transcripts in eYFP$^+$ ILCs and eYFP$^+$CD4$^+$ T cells, sorted by flow cytometry, from the lungs of *IL9*^{Cre}*R26R*^{eYFP} mice at day 12 of *N. brasiliensis* infection (n = 3). Paired samples sorted from the same mice are connected with a line. mRNA expression was normalized to *Hprt1* (encoding hypoxanthine guanine phosphoribosyltransferase). Data represent two independent experiments with similar results. Bars show mean values ± SEM.

observed an increase of total Lin$^-$Thy1.2$^+$ ILCs, which were homogeneously marked by expression of Thy1.2, in the lung tissue from day 6 on after *N. brasiliensis* infection (Fig. 2, B and C). In *Il9r*$^{-/-}$ mice, we observed a significant reduction of ILC numbers at days 9 and 12 after the infection, as compared with their WT counterparts, that was confined to the lung and not observed in the draining mediastinal LNs (MDLNs; Fig. 2, B and C; and not depicted). Importantly, the absolute numbers of CD4$^+$ T cells in the lung were similar in *Il9r*$^{-/-}$ and WT mice throughout the time course of the infection (Fig. 2 C). The increase in CD4$^+$ T cell numbers in the MDLNs was comparable in *Il9r*$^{-/-}$ mice and WT mice between days 2 and 9 and significantly higher in *Il9r*$^{-/-}$ mice at day 12 (not depicted).

Next, we wanted to address whether the observed reduction of the total ILC population was caused by a specific reduction of ILC2s. Flow cytometric analysis of the ILC lineage-defining transcription factors GATA3 and ROR-γt in the Thy1.2$^+$Lin$^-$ ILC population revealed that after *N. brasiliensis* infection the vast majority (>80%) in the lung were GATA3$^+$ ILC2s, whereas ROR-γt$^+$ ILC3s represented only a minor fraction (Fig. 2 D). Importantly, absence of the IL-9R resulted in a specific reduction of the GATA3$^+$ ILC2s in the lung, whereas the small ROR-γt$^+$ ILC3 population remained unchanged (Fig. 2, D and E).

The expression of IL-9R has been described on ILC2 precursors in the bone marrow and ILC2s in the lamina propria of the intestine of naive mice (Hoyler et al., 2012), and

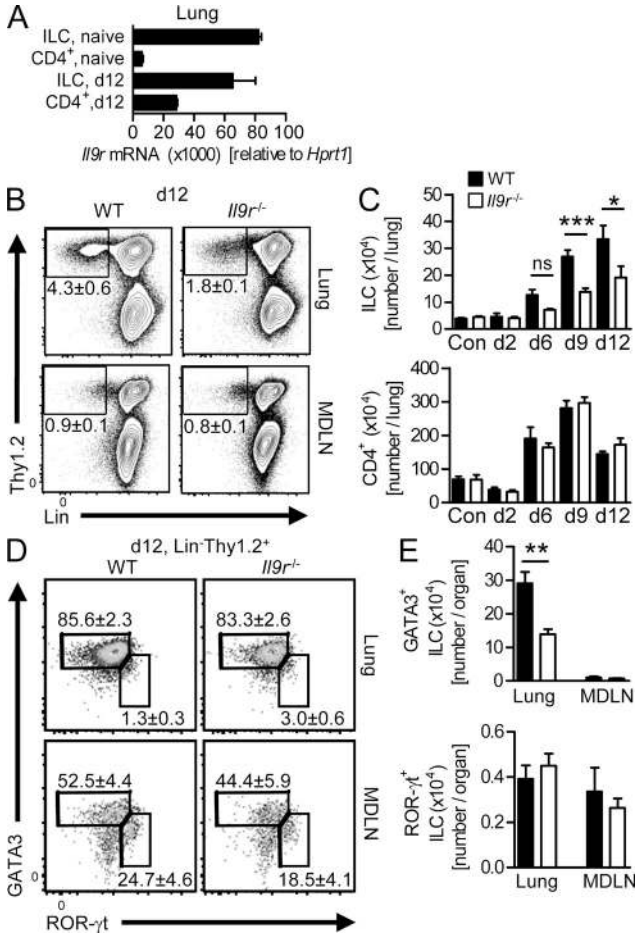

Figure 2. ILC2 accumulation in the lung tissue depends on IL-9R signaling. (A) Quantitative RT-PCR analysis of *Il9r* transcripts in Thy1.2$^+$Lin$^-$ ILCs and CD4$^+$ T cells, sorted by flow cytometry, from the lungs of naive WT mice and WT mice at day 12 of *N. brasiliensis* infection ($n = 3$). mRNA expression was normalized to *Hprt1* (encoding hypoxanthine guanine phosphoribosyltransferase). (B) Flow cytometry plots of lung and MDLN cells from WT and *Il9r*$^{-/-}$ mice at day 12 after *N. brasiliensis* infection gated on CD45$^+$ lymphoid cells. Numbers represent the percentage of Thy1.2$^+$Lin$^-$ ILCs of total cells gated ($n = 7$–8 per group; mean value ± SEM). (C) Absolute numbers of ILCs and CD4$^+$ T cells in lungs of WT and *Il9r*$^{-/-}$ mice at days 2–12 after the infection and in uninfected controls (Con; $n \geq 3$ per group; *, $P < 0.05$; ***, $P < 0.001$). (D) Flow cytometry plots of lung and MDLN cells from WT and *Il9r*$^{-/-}$ mice at day 12 after *N. brasiliensis* infection stained for surface markers and intranuclear GATA3 and ROR-γt and gated on Thy1.2$^+$Lin$^-$ ILCs. Numbers represent the percentage of transcription factor–positive ILCs of total cells gated ($n = 7$ per group; mean value ± SEM). (E) Absolute number of GATA3$^+$ and ROR-γt$^+$ ILCs in lungs and MDLNs of WT and *Il9r*$^{-/-}$ mice at day 12 of the infection (**, $P = 0.001$). Data in B–E are pooled from two independent experiments with similar results. Bars show mean values ± SEM.

we observed IL-9R expression in lung ILC2s of naive mice (Fig. 2 A), raising the question of whether this receptor is required for ILC2 maintenance in steady-state. However, the analysis of Sca-1$^+$GATA3$^+$Lin$^-$ cells in the lung, small intestine, and bone marrow of naive WT and *Il9r*$^{-/-}$ mice revealed similar numbers of these ILC2/ILC2 precursor populations (not depicted), indicating that the IL-9R is dispensable for ILC2 maintenance in the steady-state.

Cytokine production by ILC2s in the lung depends on IL-9R signaling on hematopoietic cells

To investigate the role of IL-9R expression for the function of ILC2 in the lung, we assessed the production of their hallmark cytokines IL-5 and IL-13 in *Il9r*$^{-/-}$ mice at day 12 after *N. brasiliensis* infection. The percentages and absolute numbers of IL-5– and IL-13–producing ILC2s were strongly reduced in the lung of helminth-infected *Il9r*$^{-/-}$ mice at days 6–12, whereas the IL-4, IL-5, and IL-13 production by CD4$^+$ T cells was largely uncompromised, with only a minor decrease of IL-5$^+$ T cells at day 9 (Fig. 3, A and B). Although CD4$^+$ T cells outnumbered ILC2s in the lung of *Il9r*$^{-/-}$ mice, protein levels of IL-5 and IL-13 in the lung were (significantly) reduced at days 6, 9, and 12 after the infection (Fig. 3 C). In contrast, IL-4 production was unchanged during the course of *N. brasiliensis* infection in *Il9r*$^{-/-}$ mice (Fig. 3 C), further indicating that the Th2 cell response was not affected by the absence of IL-9R signaling. Furthermore, numbers of the other T helper cell subsets, γδ T, NK, and CD8$^+$ T cells, remained unchanged in the lungs of *Il9r*$^{-/-}$ mice (not depicted).

To investigate whether IL-9 signaling on hematopoietic cells is important for maintaining ILC2s in the lung, we transferred bone marrow from either WT or *Il9r*$^{-/-}$ mice into irradiated CD45.1$^+$*Rag1*$^{-/-}$ mice, waited 6–8 wk for reconstitution, and infected them with *N. brasiliensis*. At day 12 after infection, IL-5– and IL-13–producing CD45.1-negative donor ILC2s were reduced in chimeras containing a hematopoietic compartment deficient for the IL-9R (Fig. 3, D and E). In contrast, the few radioresistant CD45.1$^+$ ILC2s remaining from the host showed similar IL-5 and IL-13 production, regardless of the bone marrow genotype. These data suggest that the maintenance of cytokine-producing ILC2s in the lung of *N. brasiliensis*–infected mice depends on their intrinsic ability to respond to IL-9.

Rapid worm expulsion depends on IL-9R signaling on hematopoietic cells

To determine the influence of IL-9R signaling on antihelminth immunity in the gut, we assessed egg production and intestinal worm burden in WT and *Il9r*$^{-/-}$ mice at different time points after *N. brasiliensis* infection (Fig. 4, A and B). Interestingly, we found increased fecal egg counts and worm numbers in the *Il9r*$^{-/-}$ mice at days 6–9. The worm burden at day 3, in contrast, was similar between both groups, indicating that the lung passage of *N. brasiliensis* was unperturbed in *Il9r*$^{-/-}$ mice and similar numbers of worms reach the intestine. However, altered kinetics of worm release from the lung in the *Il9r*$^{-/-}$ mice as a possible reason for increased intestinal worm burdens at later time points cannot be excluded. Worm counts in the irradiated *Rag1*$^{-/-}$ mice reconstituted with WT or *Il9r*$^{-/-}$ bone marrow (Fig. 3, D and E) showed that the absence of IL-9R on hematopoietic cells was sufficient to

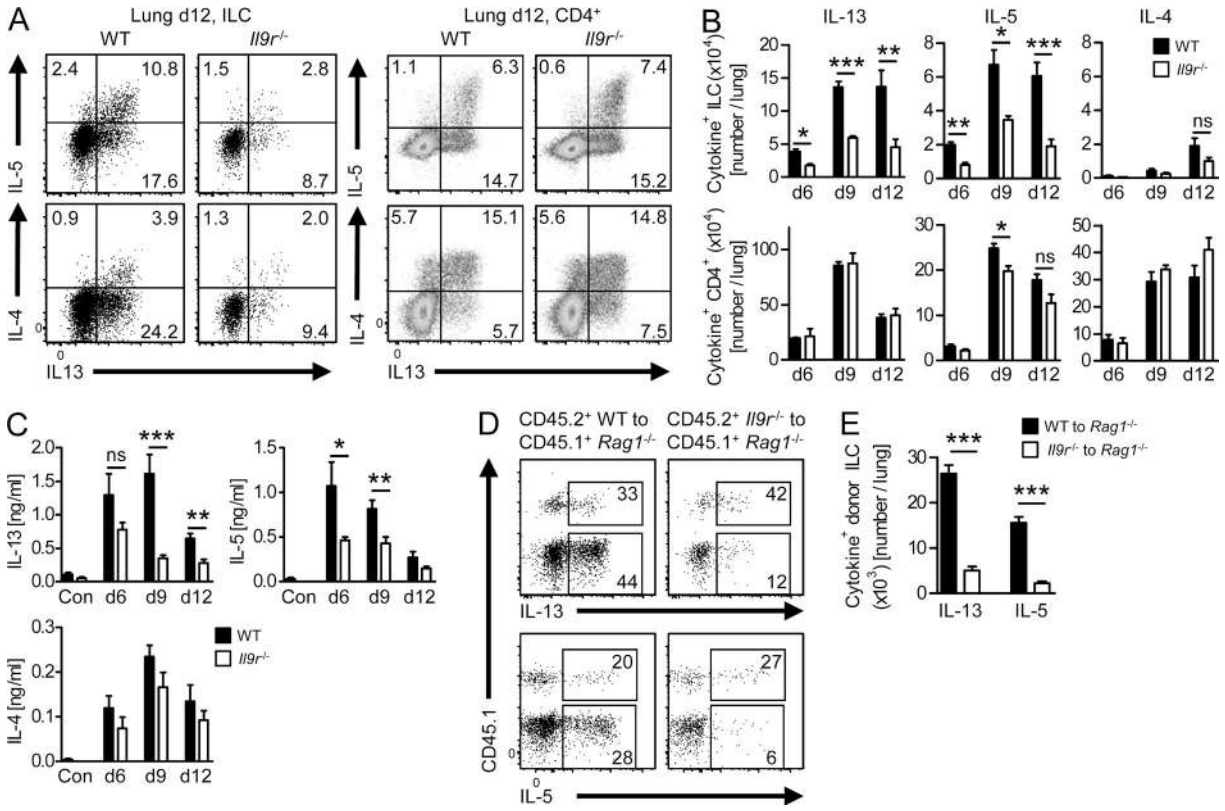

Figure 3. Cytokine production by ILC2s in the lung depends on IL-9R signaling. (A) Flow cytometry of total lung cells from *N. brasiliensis*–infected mice (day 12) restimulated with phorbol 12,13-dibutyrate and ionomycin for 2.5 h and stained intracellularly for IL-4, IL-5, and IL-13. Plots are gated for Th1.2$^+$Lin$^-$ ILCs (left) and CD4$^+$ T cells (right). Numbers indicate the percentage of cells in each quadrant. (B) Absolute number of IL-5–, IL-13–, and IL-4–positive ILC2s and CD4$^+$ T cells in WT and *Il9r*$^{-/-}$ mice at days 6–12 of the infection (n = 3–8 per group; *, P < 0.05; **, P < 0.005; ***, P < 0.001). (C) Cytokine concentrations in the lungs of WT and *Il9r*$^{-/-}$ mice at days 6, 9, and 12 of the infection and in naive controls (Con; n = 3–7 per group; *, P < 0.05; **, P < 0.01; ***, P = 0.0006). Data in B and C are representative of at least two independent experiments with similar results. (D) Flow cytometry of total lung cells from *N. brasiliensis*–infected bone marrow chimera at day 12 restimulated with phorbol 12,13-dibutyrate and ionomycin for 2.5 h and stained intracellularly for IL-5 and IL-13. Plots are gated for Thy1.2$^+$Lin$^-$ ILCs. Numbers in quadrants indicate percentage of cytokine-positive cells in the CD45.1$^-$ donor and CD45.1$^+$ recipient ILC subset. (E) Absolute number of cytokine-positive CD45.1$^-$ donor ILCs in the lungs of the respective mice (***, P < 0.0001). Data represent two independent experiments with similar results (n = 4–6). Bars show mean values ± SEM.

cause a delay in worm expulsion (Fig. 4 C). Thus, IL-9R signaling on hematopoietic cells is necessary for optimal antihelminth immunity in the gut.

IL-9 signaling affects lung tissue repair after *N. brasiliensis* infection

Type 2 immune responses have been implicated in the acute wound healing process in the lung early after *N. brasiliensis* infection (day 4; Chen et al., 2012). To investigate the impact of IL-9R signaling and ILC2s for initiation and repair of helminth-induced lung injury, we assessed lung damage parameters in WT and *Il9r*$^{-/-}$ mice at different stages after *N. brasiliensis* infection. The degree of acute lung hemorrhage and neutrophil infiltration was similar in WT and *Il9r*$^{-/-}$ mice, as indicated by equal numbers of erythrocytes and neutrophils in the bronchoalveolar lavage fluid at day 2 of the infection (Fig. 5, A and B). Although the resolution of major alveolar hemorrhage appeared to be normal in *Il9r*$^{-/-}$ mice (Fig. 5 A), we observed a strong increase in hemophagocytic macrophages, as an indicator for prolonged microbleeding (Marsland et al., 2008), in the alveolar space of *Il9r*$^{-/-}$ mice at day 12 (Fig. 5, C and D). Additionally, the emphysema-like tissue damage that is characterized by bullae formation and destruction of the regular tissue structure and develops at later stages after *N. brasiliensis* infection (Marsland et al., 2008) was dramatically increased in *Il9r*$^{-/-}$ mice at days 12 and 24 after infection (Fig. 5, E and F). Most importantly, these histopathological differences translated to a functional reduction of the lung capacity at later stages after the infection, as demonstrated by a reduced baseline tidal volume in *Il9r*$^{-/-}$ mice from day 12 onwards (Fig. 5 G). These data show that ILC2-derived IL-9 promotes damage repair and thereby ameliorates emphysema formation at chronic stages after helminth-induced lung injury.

ILCs promote lung tissue repair in *Rag1*$^{-/-}$ mice after *N. brasiliensis* infection

As ILCs have been linked to epithelial regeneration in the lung after influenza infection (Monticelli et al., 2011), we wanted

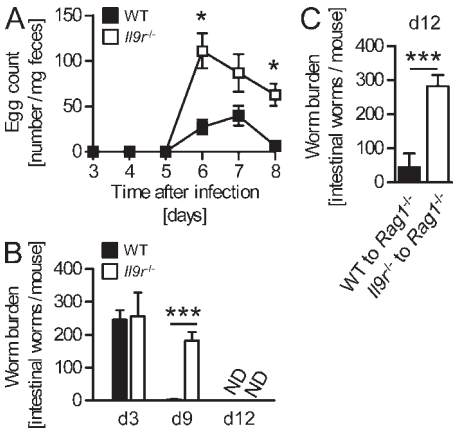

Figure 4. Delayed worm expulsion in *Il9r*$^{-/-}$ mice. (A) Egg count in feces of WT and *Il9r*$^{-/-}$ mice at days 3–8 after *N. brasiliensis* infection (n = 5–6 per time point and group; *, $P < 0.05$). (B) Worm number in the small intestine of WT and *Il9r*$^{-/-}$ mice at days 3, 9, and 12 after *N. brasiliensis* infection (n = 4–9 per time point and group; ***, $P < 0.0001$; ND, not detected). (C) Worm number in the small intestine of *N. brasiliensis*–infected bone marrow chimera at day 12 after infection (n = 7–10 per group; ***, $P < 0.0007$). Data represent two independent experiments with similar results. Bars show mean values ± SEM.

to investigate whether a reduction of lung ILCs, as observed in the *Il9r*$^{-/-}$ mice, can lead to impaired lung damage repair after *N. brasiliensis* infection. To address this question, we used an anti-Thy1.2 antibody to deplete ILCs in *N. brasiliensis*–infected *Rag1*$^{-/-}$ mice. In these experiments, ILCs were identified by flow cytometry for lineage markers and IL-7R because the Thy1.2 staining was found to be unreliable in anti-Thy1.2 antibody–treated mice (Fig. 6 A). Anti-Thy1.2 antibody treatment resulted in a ∼50% reduction in ILC numbers at day 12 after *N. brasiliensis* infection (Fig. 6, A and B). In line with the hypothesis that ILC reduction leads to impaired lung tissue restoration, we observed a significant increase in the emphysema-like lung damage in ILC-depleted *Rag1*$^{-/-}$ mice as compared with the isotype-treated controls (Fig. 6 C). Thus, ILCs contribute to damage repair after helminth-induced lung injury.

IL-9 signaling promotes eosinophil recruitment and alternative activation of macrophages after *N. brasiliensis* infection

Eosinophil recruitment is a hallmark of type 2 responses in the lung, and IL-33–induced ILC2 expansion has been shown to contribute to lung eosinophilia in *Strongyloides venezuelensis* induced lung inflammation (Yasuda et al., 2012). Furthermore, it has been shown recently that eosinophils promote tissue regeneration after muscle injury (Heredia et al., 2013). In line with the reduced ILC2 numbers and IL-5 levels, we found significantly reduced eosinophil numbers (identified as CD11b^{+}Ly6G^{-}SiglecF^{+}CD11c^{-}) in the lungs of *Il9r*$^{-/-}$ mice at days 6–12 after *N. brasiliensis* infection (Fig. 7, A and B). Because histological analysis at day 12 after infection suggested differences in the macrophage populations (Fig. 5, C and D), we also quantified alveolar and conventional macrophages in the lungs of WT in *Il9r*$^{-/-}$ mice after *N. brasiliensis* infection (Fig. 7, A and C–E). Interestingly, we found increased numbers of CD11b^{+}Ly6G^{-}SiglecF^{+}CD11c^{hi} alveolar macrophages at days 9 and 12 after *N. brasiliensis* infection (Fig. 7 C), probably representing the increase in heme-laden macrophages observed in the Prussian blue staining. The total number of SiglecF^{-}Ly6G^{-}CD11b^{hi}F4/80^{+} conventional macrophages, in contrast, was unaltered in *Il9r*$^{-/-}$ mice at days 6–12 after *N. brasiliensis* infection (Fig. 7, D and E), as was the relation of Ly6C^{hi} inflammatory monocytes to Ly6C^{lo} resident macrophages (Jenkins et al., 2011) at these time points (not depicted). To address the potential influence of IL-9R signaling on the activation status of conventional macrophages, we sorted SiglecF^{-}Ly6G^{-}CD11b^{hi}F4/80^{+} macrophages from the lungs of WT and *Il9r*$^{-/-}$ mice and assessed expression of markers for alternative activation (Fig. 7 F). This analysis showed significantly reduced levels of *Retnla* (RELM-α) mRNA in macrophages from *Il9r*$^{-/-}$ mice, whereas *Arg1* (Arginase 1) and *Chi3l3* (Ym-1) levels were also lower, but the reduction failed to reach statistical significance. Importantly, the *Il9r* mRNA levels in lung macrophages were very low (close to the detection limit; not depicted), indicating that the effect of IL-9R deficiency on macrophage activation status is indirect, probably via the reduced IL-13 levels found in the lungs of *Il9r*$^{-/-}$ mice. Next, we addressed the abundance and function of goblet cells and mast cells in *Il9r*$^{-/-}$ mice by histological analysis and expression analysis of goblet cell– and mast cell–related transcripts in total lung RNA extracts (Fig. 7, G–K). These analyses showed similar goblet cell hyperplasia and mast cell accumulation in WT and *Il9r*$^{-/-}$ mice at days 12 and 9 (not depicted) and revealed only a modest reduction of the mucin *Muc5ac* and the mast cell protease *Mcpt1* in *Il9r*$^{-/-}$ mice that did not reach statistical significance (Fig. 7, G–K). Furthermore, the mRNA expression of the matrix metalloproteinases MMP12 and MMP13, which play a role in tissue remodeling, was induced similarly in WT and *Il9r*$^{-/-}$ mice (Fig. 7 L). Collectively, these data indicate that IL-9 signaling, most likely by promoting ILC2 accumulation and enhancing production of IL-5 and IL-13 by ILC2s, can influence the function of eosinophils and alternatively activated macrophages that contribute to damage repair mechanisms in the lung.

Increased expression of ILC2-derived amphiregulin after *N. brasiliensis* infection depends on IL-9 signaling

In addition to IL-9, IL-13, and IL-5, ILC2s produce the epidermal growth factor family member amphiregulin and thereby promote the regeneration of bronchiolar epithelium after influenza infection in *Rag1*$^{-/-}$ mice (Monticelli et al., 2011). To explore a potential role of ILC2-derived amphiregulin after *N. brasiliensis*–induced lung injury, we purified *IL9*^{Cre}eYFP^{+} lung ILC2s at day 12 after the infection and assessed amphiregulin mRNA expression by quantitative RT-PCR. Indeed, we found high expression of amphiregulin mRNA in these lung ILC2s, whereas amphiregulin expression

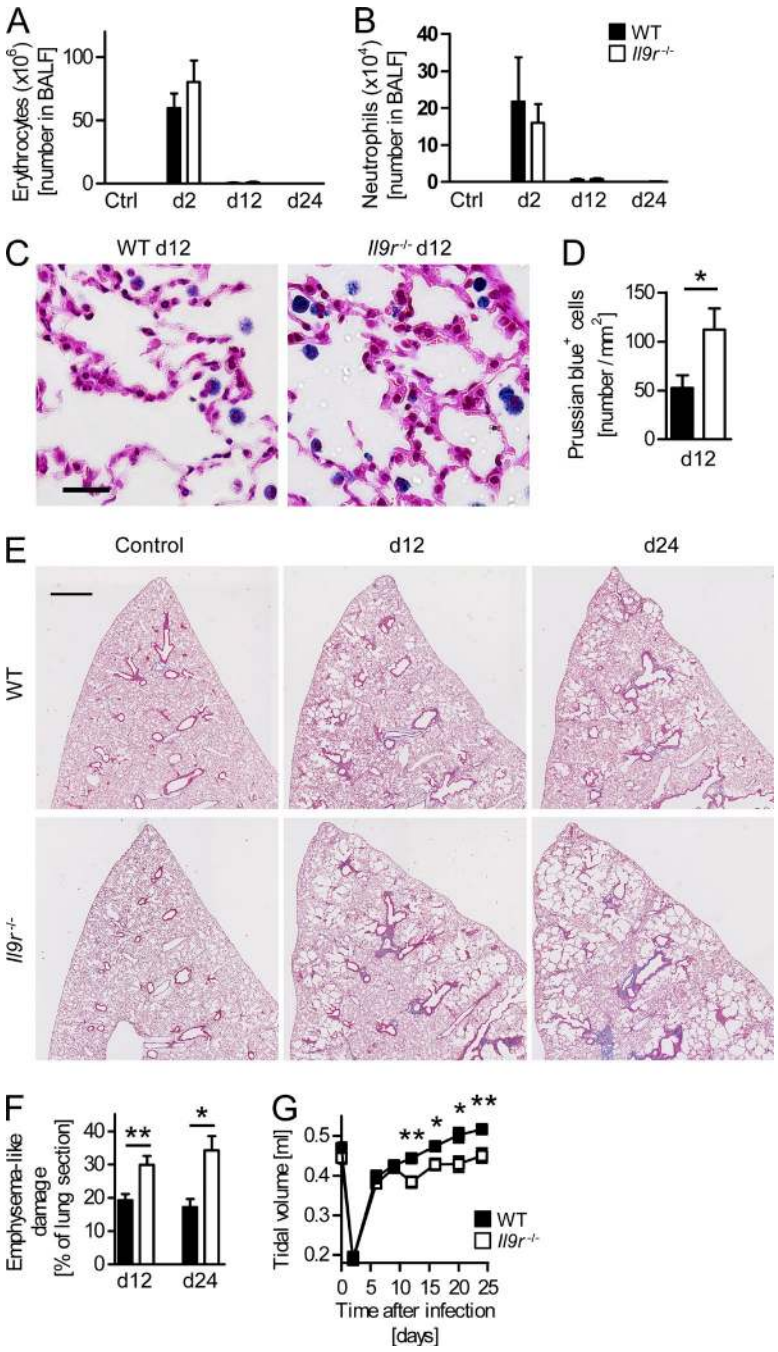

Figure 5. IL-9 is required for lung damage repair. (A and B) Number of erythrocytes (A) and neutrophils (B) in the bronchoalveolar lavage fluid (BALF) of WT and *Il9r*$^{-/-}$ mice at days 2, 12, and 24 of *N. brasiliensis* infection and in naive controls (Ctrl; n = 6–10 for experimental groups and n = 3–5 for controls). (C and D) Prussian blue staining for iron deposits in lung sections (C) and quantification of Prussian blue–positive (= hemophagocytic) macrophages (D) in *N. brasiliensis*–infected WT and *Il9r*$^{-/-}$ mice at day 12 (n = 7–8 per group; *, P = 0.04). (E and F) Masson's trichrome staining of lung sections (E) and histological quantification of the emphysema-like lung damage (F) in lungs of WT and *Il9r*$^{-/-}$ mice at days 12 and 24 after the infection (n = 3–8 per group; *, P = 0.03; **, P = 0.007). Bars: (C) 25 µm; (E) 100 µm. (G) Tidal volume of WT and *Il9r*$^{-/-}$ mice shortly before and at different time points after the infection with *N. brasiliensis* (n = 5–18 per group; *, P = 0.02; **, P = 0.005). Data represent at least two independent experiments with similar results. Bars show mean values ± SEM.

in *IL9*^{Cre}eYFP^{+} T cells isolated from the same *IL9*^{Cre}*R26R*^{eYFP} reporter mice was significantly lower (Fig. 8 A). Comparison of transcript levels between *IL9*^{Cre}eYFP^{+} ILC2s and *IL4*-GFP^{+} Th2 cells from *IL4*-GFP (4get) mice, as well as eosinophils and macrophages all sorted from the lung at day 12 after infection showed the highest amphiregulin expression in ILC2s (Fig. 8 A). Interestingly, the RT-PCR analysis of ILC2s, sorted from the lung at day 12 after infection, indicated that *Il9r*$^{-/-}$ ILCs from infected mice expressed similar levels of amphiregulin mRNA as their WT counterparts (Fig. 8 B). However, the reduction of ILC2 numbers in *Il9r*$^{-/-}$ mice at day 12 after *N. brasiliensis* infection resulted in strongly reduced total amphiregulin mRNA levels in the lungs (Fig. 8 C). Thus, ILC2s appear to be the major source of amphiregulin in the infected lung and might use this mediator to promote tissue repair after *N. brasiliensis*–induced lung injury.

IL-9 is dispensable for ILC proliferation

One possible mechanism of how IL-9 might promote ILC2 accumulation in the lung is by enhancing their proliferation in *N. brasiliensis*–infected mice. We therefore assessed Ki67

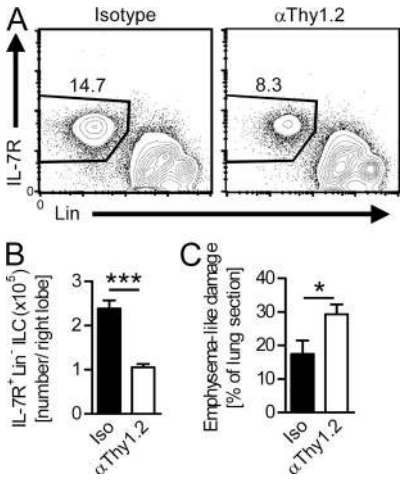

Figure 6. ILCs promote lung tissue repair after *N. brasiliensis* infection. (A) Flow cytometry plots of lung cells from isotype and α-Th1.2–treated mice at day 12 after *N. brasiliensis* infection gated on CD45$^+$ lymphoid cells. Numbers represent the percentage of IL-7R$^+$Lin$^-$ ILCs of total cells gated. (B) Absolute numbers of ILCs in the right lung of isotype and α-Th1.2–treated mice 12 d after the infection (n = 6–10; ***, P < 0.0001). (C) Histological quantification of the emphysema-like lung damage in lungs of isotype and α-Th1.2–treated mice at day 12 (n = 6–8 per group; *, P = 0.03). Data represent two independent experiments with similar results. Bars show mean values ± SEM.

expression in lung ILC2s, as a marker for cells that are in active phases of the cell cycle. As expected, the percentage of Ki67$^+$ ILC2s in the lungs of helminth-infected mice increased over time (Fig. 9, A and B), indicating an accumulation of activated cells. Comparison of the numbers of Ki67$^+$ ILC2s in WT and *Il9r*$^{-/-}$ mice at day 12 after infection demonstrated a reduction of Ki67$^+$ ILC2s in the absence of IL-9R signaling (Fig. 9 C). However, the 5′-ethynyl-2′-deoxyuridine (EdU) incorporation rate analyzed 2 h after i.v. injection of the substance, as a direct indicator of actual in situ proliferation, was similar in ILC2s from the lung and Thy1.2$^+$Lin$^-$ cells in the MDLNs and bone marrow of WT and *Il9r*$^{-/-}$ mice at the peak of IL-9 expression (day 9; Fig. 9, D and E). Interestingly, Thy1.2$^+$Lin$^-$ ILCs in the MDLNs, being ∼50% GATA3$^+$ ILC2s (Fig. 2 D), showed a much higher EdU incorporation rate than lung ILC2s irrespective of IL-9R expression (Fig. 9, D and E). This suggests that ILC2 expansion in the later phase of the infection might take place in the draining LNs, followed by recruitment of the cells to the target organ. Thy1.2$^+$Lin$^-$ cells in the bone marrow, which were ∼80% GATA3$^+$ ILC2/ILC2 precursors (not depicted; Hoyler et al., 2012), showed a baseline proliferation rate that was not changed after *N. brasiliensis* infection. These data indicate that proliferation of ILC2s in response to *N. brasiliensis* infection is not compromised by the lack of IL-9R signaling.

IL-9 protects ILC2s from apoptosis

To investigate a direct effect of IL-9 on ILC2s, we isolated ILC2s from the lungs of *N. brasiliensis*–infected mice at day 12 after the infection and cultured them in the presence or absence of IL-9. Supplementing the culture medium with IL-9 resulted in strongly increased production of IL-5 and IL-13 in WT but not in *Il9r*-deficient ILC2s (Fig. 10 A). As we had previously hypothesized IL-9 might mediate biological functions by promoting the survival of a variety of cell types (Wilhelm et al., 2012), we investigated the possibility that enhanced cytokine expression by cultured ILC2s in the presence of IL-9 could be a consequence of their increased IL-9–mediated survival. To address this issue, we assessed the amount of live cells in the ILC2 cultures by Annexin V and 7-amino-actinomycin D (7AAD) staining. The highly activated ILC2 population isolated at the height of lung inflammation at day 12 showed a large proportion of apoptotic cells after 2 d of culture, indicating the strong predisposition of this cell population to undergo apoptosis. The presence of IL-9 in the culture medium, however, was able to rescue a significant proportion of ILC2s from apoptotic cell death (Fig. 10, B and C). Additionally, the addition of IL-9 resulted in an increased forward scatter profile of ILC2s, indicating an activated blast stage (Fig. 10 C). To assess the number of apoptotic cells in the lung in vivo, we stained tissue sections for expression of the apoptosis marker cleaved caspase-3. Indeed, *N. brasiliensis*–infected *Il9r*$^{-/-}$ mice showed increased numbers of cleaved caspase-3–positive lymphoid cells in the lung infiltrates (Fig. 10, E and F). To further explore potential mechanisms of how IL-9 might protect ILC2s from apoptotic cell death in vivo, we purified ILC2s from the lungs of WT and *Il9r*$^{-/-}$ mice at the peak of IL-9 expression (day 9) and assessed mRNA expression of antiapoptotic proteins that have previously been linked to IL-9–mediated survival in different cell types in vitro (Richard et al., 1999; Rebollo et al., 2000; Fontaine et al., 2008). Whereas BCL2 and BCLXL expression were unchanged, we found a significant reduction of BCL3 expression in *Il9r*$^{-/-}$ ILCs (Fig. 10 G), a survival factor which has been shown to be directly regulated by IL-9 signaling (Richard et al., 1999). Expression of BCL2, which is induced by γ_c cytokines such as IL-7 and IL-2 (Deng and Podack, 1993; von Freeden-Jeffry et al., 1997) was unaffected in line with unimpaired surface expression of IL-7R and CD25 on *Il9r*$^{-/-}$ ILC2s (Fig. 10 H). Collectively, these data suggest that IL-9 is an autocrine factor that promotes ILC2 survival by inducing the expression of the antiapoptotic protein BCL3, thereby maintaining their functional activity in vivo.

DISCUSSION

For many years IL-9 was considered to be a cytokine produced by T cells and involved in Th2 responses. IL-9 acts on a wide spectrum of hematopoietic and nonhematopoietic cell types (Goswami and Kaplan, 2011); however, its exact function remained elusive. Several publications provided evidence that in the context of type 2 responses, IL-9 promotes IL-5 and IL-13 production (at that time attributed mainly to Th2 cells) in the lung (Temann, Ray, and Flavell, 2002) and gut-associated lymphoid tissue (Fallon et al., 2000). This suggested an indirect action of IL-9 via promotion of other cytokines.

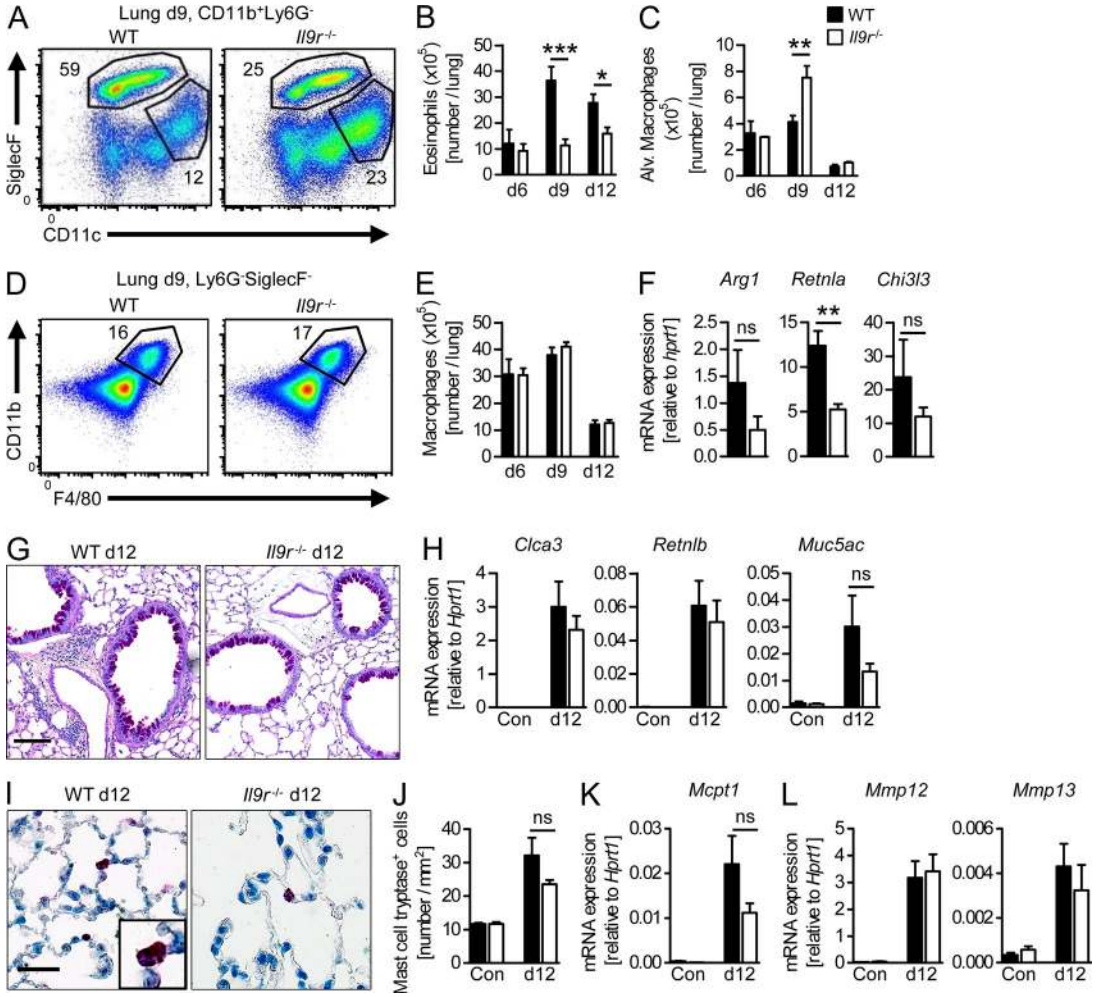

Figure 7. IL-9 signaling promotes eosinophil recruitment and alternative activation of macrophages. (A and D) Flow cytometry plots of lung cells from WT and *Il9r*$^{-/-}$ mice at day 9 after *N. brasiliensis* infection gated on CD11b^{+}Ly6G^{-} cells (A) and Ly6G^{-}SiglecF^{-} cells (D). Numbers represent the percentage of SiglecF^{+}CD11c^{-} eosinophils (A), SiglecF^{+}CD11c^{hi} alveolar macrophages (A), and conventional CD11b^{hi}F4/80^{+} macrophages/monocytes (D). (B, C, and E). Absolute numbers of eosinophils (B), alveolar macrophages (C), and macrophages/monocytes (E) at days 6–12 in the lung of WT and *Il9r*$^{-/-}$ mice ($n \geq 3$ per group; *, P = 0.01; **, P = 0.003; ***, P < 0.004). (F) Quantitative RT-PCR analysis of mRNA transcripts in conventional lung macrophages, sorted by flow cytometry, from the lungs of WT and *Il9r*$^{-/-}$ mice at day 12 of *N. brasiliensis* infection ($n = 5$; **, P = 0.003). (G) Representative periodic acid–Schiff staining of lung sections in WT and *Il9r*$^{-/-}$ mice at day 12 of the infection. (H) Quantitative RT-PCR analysis of goblet cell–related transcripts in total lung RNA samples at day 12 after infection of WT and *Il9r*$^{-/-}$ mice and in naive controls (Con). (I and J) Representative immunohistochemical staining of lung sections for mast cell tryptase (I) and quantification of mast cell tryptase^{+} cells (J) in WT and *Il9r*$^{-/-}$ mice at day 12 of the infection. The inset shows granular mast cell tryptase staining at a higher magnification. Bars: (G) 100 µm; (I) 25 µm. (K and L) Quantitative RT-PCR analysis of mRNA transcripts in total lung RNA samples at day 12 after infection of WT and *Il9r*$^{-/-}$ mice and in naive controls (Con; H–L: $n = 8$–9 for day 12, $n = 3$ for controls). mRNA expression was normalized to *Hprt1* (encoding hypoxanthine guanine phosphoribosyltransferase). Data represent at least two independent experiments with similar results. Bars show mean values ± SEM.

Indeed, the spontaneous airway inflammation observed in mice with transgenic overexpression of IL-9 was found to be independent of IL-9R expression in nonhematopoietic cells (Steenwinckel et al., 2007), suggesting that the role of IL-9 might be that of a regulatory cytokine rather than a direct effector cytokine. This is further illustrated by the fact that the pulmonary phenotype of *Il9* transgenic mice is abolished if these mice are crossed to an IL-13–deficient background (Steenwinckel et al., 2007; Temann et al., 2007). Strikingly, pulmonary inflammation and IL-13 production in *Il9* transgenic mice were not abrogated, but in contrast even enhanced on a T cell– and B cell–deficient background (Temann et al., 2007), strongly suggesting that an innate cell type and not Th2 cells is one of the major targets of IL-9.

Recently, the generation of an IL-9 fate reporter mouse strain (*IL9*^{Cre}*R26R*^{eYFP} mice) enabled us to identify ILC2s as potent producers of IL-9 in vivo in a model of papain-induced lung inflammation (Wilhelm et al., 2011). We could further show that IL-5 and IL-13 expression in ILC2s is regulated by IL-9, albeit the underlying mechanism and the functional importance of ILC2-derived IL-9 was not addressed (Wilhelm et al., 2011).

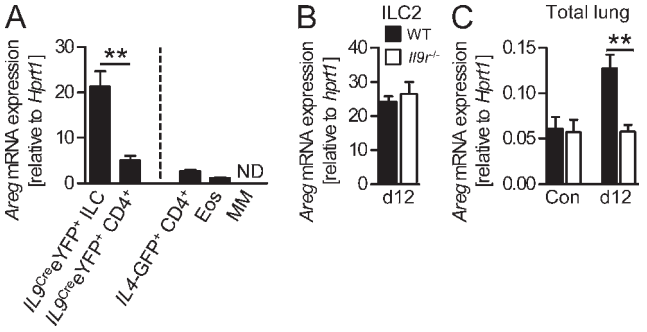

Figure 8. Expression of ILC2-derived amphiregulin depends on IL-9 signaling. (A) Quantitative RT-PCR analysis of amphiregulin (*Areg*) transcripts in *IL9*^{Cre}eYFP$^+$ ILC2s, *IL9*^{Cre}eYFP$^+$ CD4$^+$ T cells, *IL4*-GFP$^+$ Th2 cells, eosinophils (Eos), and macrophages (MM) purified at day 12 of the infection from the lungs of *IL9*^{Cre}*R26R*^{eYFP}, *4get* (*IL4*^{GFP}), and WT mice (n = 3–4 per group; **, P = 0.004; ND, not detected). (B and C) Quantitative RT-PCR analysis of amphiregulin (*Areg*) transcripts in sorted ILC2s (n = 4–5; B) and in total lung RNA samples (C) at days 9 and 12 after infection of WT and *Il9r*$^{-/-}$ mice and in naive controls (Con; n = 8–9 for day 12, n = 3 for controls; **, P = 0.004). Data are representative for two independent experiments. mRNA expression was normalized to *Hprt1* (encoding hypoxanthine guanine phosphoribosyltransferase). Bars show mean values ± SEM.

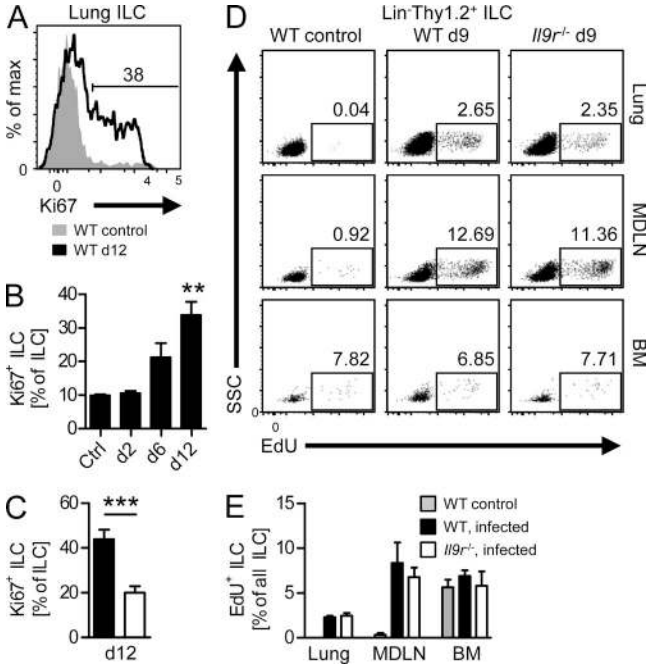

Figure 9. IL-9 is dispensable for ILC proliferation. (A) Flow cytometry of intranuclear Ki67 expression in lung ILCs from uninfected WT control mice and mice at day 12 after *N. brasiliensis* infection. The number represents the percentage of Ki67$^+$ ILC2s at day 12. (B) Percentage of Ki67$^+$ lung ILC2s at different time points (days 2–12) after *N. brasiliensis* infection and in naive controls (Ctrl; n = 3–4 per time point; **, P = 0.004 vs. control). (C) Percentage of Ki67$^+$ ILC2s in the lungs of WT and *Il9r*$^{-/-}$ mice at day 12 of the infection (n = 5–7 per group; ***, P = 0.0007). (D) Flow cytometric assessment of EdU incorporation by Lin$^-$Thy1.2$^+$ ILCs in the lung, MDLNs, and bone marrow of uninfected WT controls, infected WT, and infected *Il9r*$^{-/-}$ mice at day 9, 2 h after i.v. injection of 1 mg EdU per mouse. Numbers represent EdU$^+$ cells in the percentage of total ILCs. (E) Percentage of EdU$^+$ (= proliferated within 2 h) ILCs in the lung, MDLNs, and bone marrow of the three groups (n = 4–5). Data in C–E represent two independent experiments with similar results. Bars show mean values ± SEM.

Here we show, using a model of *N. brasiliensis* infection in mice, that IL-9 is an ILC2-derived cytokine that critically amplifies the function of IL-13– and IL-5–producing ILC2s by promoting their survival and activation in a positive autocrine feedback loop. Furthermore, we show for the first time that a reduction of lung ILC2s in *Il9r*$^{-/-}$ mice leads to reduced levels of IL-13, IL-5, and amphiregulin, reduced eosinophil recruitment, and alternative activation of macrophages and consequently to impaired lung tissue repair, even though the Th2 response in these mice is intact.

In contrast to the IL-7R (Hoyler et al., 2012), expression of IL-9R was dispensable for maintenance of ILC2s in naive mice, indicating that IL-9 provides a survival signal only for activated ILC2s. Here we identify the antiapoptotic protein BCL3 as a potential mediator for IL-9–mediated protection of activated ILC2s from apoptosis. Interestingly, BCL3 has been described to depend directly on IL-9–mediated Jak/STAT signaling but was not induced by IL-2 (Richard et al., 1999). Furthermore, BCL3 has been shown to promote the survival of T cells in vitro (Rebollo et al., 2000; Bauer et al., 2006). In contrast to BCL3, the expression of the antiapoptotic factor BCL2 that is induced by other γ_c receptor cytokines like IL-2 and IL-7 (Deng and Podack, 1993; von Freeden-Jeffry et al., 1997) was not changed in *Il9r*$^{-/-}$ ILC2s, indicating that IL-9 might use a survival pathway distinct from the other γ_c receptor cytokines in vivo.

It has been postulated that the type 2 immune response induced by helminth infections, apart from being instrumental in effective antihelminth immunity, is also required for the wound-healing process that is critical for limiting the extensive tissue damage that these multicellular pathogens often cause while migrating through the host (Allen and Maizels, 2011). In line with this, the absence of the IL-4Rα chain, abolishing both IL-4 and IL-13 signaling, in mice with *N. brasiliensis* infection greatly impaired the resolution of the acute lung hemorrhage caused by this parasite in an early stage (day 4) of the infection (Chen et al., 2012). However, the cell type responsible for this early production of type 2 cytokines in response to the helminth infection was not identified in this study (Chen et al., 2012).

Apart from the acute lung injury observed in *N. brasiliensis*–infected mice, these mice develop chronic histopathological alterations of the lung tissue that resemble lung emphysema, a common end-stage of chronic obstructive pulmonary disease in humans (Marsland et al., 2008). Although previous studies described an accumulation of ILC2s in the lungs of *N. brasiliensis*–infected mice predominantly at later time points (after day 7; Price et al., 2010; Liang et al., 2012), the role of these cells in the chronic tissue remodeling process

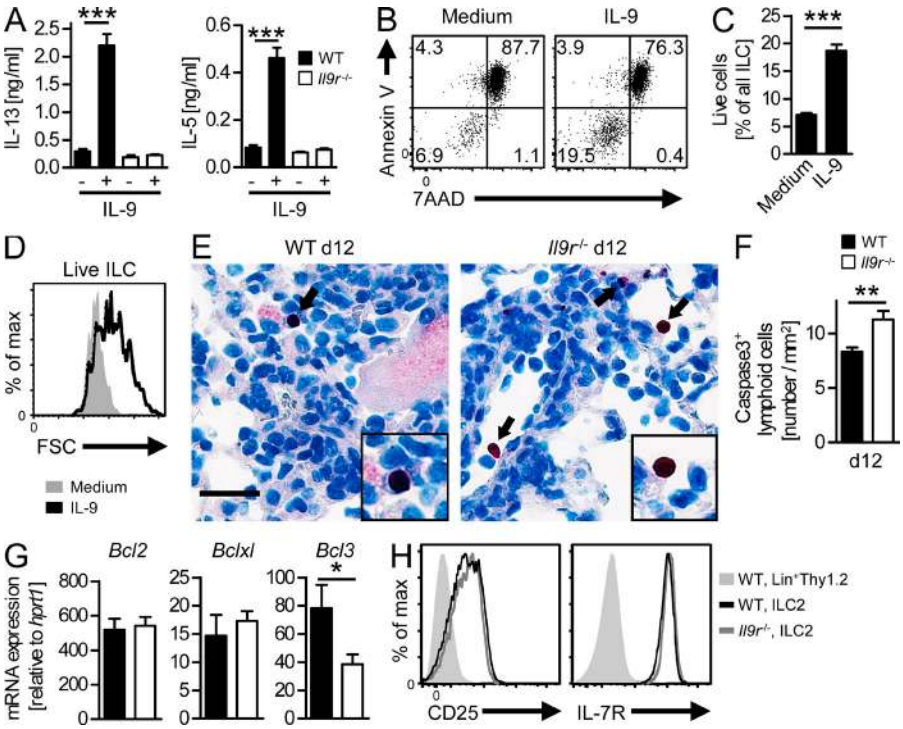

Figure 10. IL-9 enhances cytokine production and survival of lung ILCs. (A) IL-13 and IL-5 protein concentration in the culture supernatant of ILC2s, sorted by flow cytometry, from the lungs of WT and *Il9r*$^{-/-}$ mice at day 12 after *N. brasiliensis* infection and cultured for 2 d with or without IL-9 (50 ng/ml in all experiments; $n = 3$–4 per group; ***, $P < 0.0001$). (B) Flow cytometry of lung ILC2s, sorted by flow cytometry, from infected WT mice (day 12) after 2 d of culture with and without IL-9. Numbers indicate the percentage of cells in each quadrant. (C) Percentage of live ILC2s (Annexin V^{-}7AAD^{-}) at day 2 of culture ($n = 3$–4 per group; ***, $P = 0.0003$). (D) Flow cytometry for forward scatter (FSC) gated on live ILC2s after 2 d of culture with and without IL-9. (E and F) Immunohistochemical staining of lung sections for cleaved caspase-3 (E) and quantification of cleaved caspase-3–positive lymphoid cells (F) in lungs of WT and *Il9r*$^{-/-}$ mice at day 12 after the infection ($n = 7$–8 per group; **, $P = 0.005$). Insets show caspase-3 staining at a higher magnification. Arrows indicate caspase-3–positive cells. Bar, 25 µm. Data represent at least two independent experiments with similar results. (G) Quantitative RT-PCR analysis of mRNA expression of antiapoptotic proteins in ILC2s, sorted by flow cytometry, from the lungs of WT and *Il9r*$^{-/-}$ mice at day 9 of *N. brasiliensis* infection ($n = 6$; *, $P = 0.04$). Bars show mean values ± SEM. (H) Flow cytometry for CD25 and IL-7R expression on ILC2s from the lungs of *N. brasiliensis*–infected WT and *Il9r*$^{-/-}$ mice.

after the acute wound closure has not been addressed so far. In line with these studies, we observed a striking increase of ILC2s in the lung after day 6 of the infection compared with naive mice.

The involvement of ILC2s in maintaining lung tissue integrity had so far only been addressed in mice lacking an adaptive immune system (Monticelli et al., 2011). Therefore, the importance of ILC2s for total cytokine production and tissue repair in comparison with Th2 cells in immunocompetent mice remained unknown. A detailed characterization of ILC populations and T cell subsets in the lung and draining MDLNs of *Il9r*$^{-/-}$ mice infected with *N. brasiliensis* revealed an organ- and cell type–specific reduction of lung ILC2s caused by their impaired survival in the absence of IL-9R signaling. Using this model, we demonstrate that, even though the acute resolution of alveolar hemorrhage appeared unimpaired in *Il9r*$^{-/-}$ mice, the absence of IL-9R signaling, most likely caused by the reduction of the ILC2 population, resulted in increased emphysema formation and reduced lung function in the chronic stage after the infection. Furthermore, we show that treatment of *Rag1*$^{-/-}$ mice with a depleting α-Thy1.2 antibody partially reduces ILC numbers in the lungs after *N. brasiliensis* infection and leads to an increase in emphysematous pathology, supporting an important role for ILCs in damage repair after helminth-induced lung inflammation.

ILC2s produce IL-5, IL-9, IL-13, and potentially other mediators that may enhance damage repair by either directly acting on tissue-resident cells or by changing the abundance and/or activation status of other immune cells. We show here that, in line with reduced IL-5 and IL-13 levels, the absence of IL-9R signaling reduces eosinophil recruitment, increases the presence of alveolar macrophages, and impairs alternative activation of interstitial macrophages. As macrophages sorted from the lung did not express the IL-9R, this effect is likely to be mediated indirectly via the reduced IL-13. Both eosinophils and macrophages have recently been shown to promote tissue repair (Chen et al., 2012; Heredia et al., 2013), and macrophages are known to play an important role in emphysematous lung pathology after *N. brasiliensis* infection (Heitmann et al., 2012). However, it is possible that the slight reduction in the number of IL-5^{+} CD4^{+} T cells in *Il9r*$^{-/-}$ animals contributes to the effect of IL-9R deficiency, reduced IL-5 levels, and eosinophil recruitment.

As an important part of the type 2 response, goblets cells and mast cells are two other potential target cell populations of ILC2-produced mediators. However, goblet cell hyperplasia

and mast cell accumulation in the lung were only slightly reduced in *Il9r*$^{-/-}$ mice in the late phase after *N. brasiliensis*–induced injury, arguing against a major role of IL-9/ILC2 for these cell types in this model.

A previous study in mice lacking T and B cells (Monticelli et al., 2011) identified ILC2s as an important source of amphiregulin, a member of the epidermal growth factor family which promotes regeneration of the bronchiolar epithelium after acute virus-induced epithelial cell death. Amphiregulin is also produced by mouse Th2 cells (Zaiss et al., 2006), so that the relative contribution of ILC2s compared with Th2 to the production of this mediator, as well as its functional importance for lung repair in immunocompetent mice remained unknown. Here we show in mice with a largely uncompromised immune system that ILC2s are an important source of amphiregulin in chronic lung inflammation and that, along with the reduction in ILC2s, the absence of IL-9R signaling prevents up-regulation of amphiregulin expression in the lung at later stages after helminth-induced lung injury. It is conceivable that ILC2s might use this mediator to promote tissue repair after *N. brasiliensis*–induced lung injury.

Interestingly, the deficiency in IL-4, IL-5, or IL-13 signaling alone appears to have no effect on *N. brasiliensis*–induced emphysema formation in BALB/c mice (Marsland et al., 2008). Although comparative studies of the regulation of emphysema formation between the C57BL/6 and BALB/c background are missing, the fact that we observe increased emphysema formation in *Il9r*$^{-/-}$ mice suggests that IL-9 is an important regulator in the process of chronic lung remodeling by enhancing ILC2 survival. Moreover, IL-9 production by ILC2s has recently been confirmed in human CD127^{+}CRTH2^{+} ILC2s (Mjösberg et al., 2012), underlining the importance of this cytokine for ILC2 function also in humans.

The relevance of this autocrine feedback loop that promotes ILC2 accumulation in the tissue might lie in a need to tightly control this potentially harmful cell population that can cause allergic airway inflammation if left unchecked. These highly activated ILC2s are prone to apoptotic cell death and might use the transient expression of IL-9 as a mechanism to prolong their survival and delay their clearance from the tissue.

MATERIALS AND METHODS

Mice. *IL9*^{Cre}*R26R*^{eYFP} (Wilhelm et al., 2011), *Il9r*$^{-/-}$ (Steenwinckel et al., 2007) and *4get* (*IL4*^{GFP}; Mohrs et al., 2005) mice on a C57BL/6 background, C57BL/6 WT mice, and C57BL/6 CD45.1^{+}*Rag1*$^{-/-}$ and CD45.2^{+}*Rag1*$^{-/-}$ mice were bred in the animal facility at the National Institute for Medical Research (NIMR) under specific pathogen–free conditions. All genetically modified strains were backcrossed to C57BL/6 at the NIMR for 10 generations. For bone marrow transplantation, CD45.1^{+}*Rag1*$^{-/-}$ mice were sublethally irradiated (8 Gray), injected i.v. with 4 × 10^{6} bone marrow cells from CD45.2^{+} donors, and allowed to reconstitute for at least 6 wk. Adult (>6 wk) male and female mice with their respective age- and gender-matched control were used in all experiments. All animal experiments were performed according to institutional (NIMR Animal Welfare and Ethical Review Panel) and the UK Home Office regulations (Project license 80/2506).

***N. brasiliensis* infection.** The *N. brasiliensis* life cycle (mouse adapted; provided by R. Maizels, University of Edinburgh, Edinburgh, Scotland, UK) was maintained at the NIMR. Infective *N. brasiliensis* L3 stage larvae were isolated from fecal cultures by using a modified Baermann apparatus as described in detail elsewhere (Camberis et al., 2003). L3 larvae were washed four times in 15 ml PBS, counted, and injected subcutaneously in the neck (500 L3 larvae per mouse) under isoflurane anesthesia.

Antibody treatment. For depletion of ILCs, *Rag1*$^{-/-}$ mice were injected i.p. with 300 µg anti-Thy1.2 antibody (clone 30H12; Bio X Cell) every other day, starting 1 d before the *N. brasiliensis* infection. Control mice received 300 µg isotype control (clone LTF-2; Bio X cell) at the same time points.

Cell isolation. For isolation of lung cells, lungs were finely minced, digested in IMDM (Sigma-Aldrich) with 0.4 mg/ml Liberase (Roche) for 45 min and meshed through a 70-µm cell strainer. LNs were meshed through a 70-µm strainer. Bone marrow cells were flushed out from the femur and tibiae with a syringe and passed through a 70-µm strainer. Small intestines were thoroughly rinsed with PBS, cut in 0.5–1-cm pieces, and shaken at 200 rpm for 30 min in PBS containing 10% fetal calf serum, 1 mM Pyruvate, 20 µM Hepes, 10 mM EDTA, 100 U/liter penicillin, 100 mg/ml streptomycin, 10 µg/ml Polymyxin B, and 2 mM DTT to remove epithelial cells and intraepithelial lymphocytes. After digestion for 1 h at 37°C in IMDM (supplemented with 5% fetal calf serum, 2 mM L-glutamine, 50 nM β-mercapto-ethanol, 100 U/liter penicillin, and 100 mg/ml streptomycin) with 1 mg/ml Collagenase (Roche) and 10 U/ml DNase I (Sigma-Aldrich), gut tissue was meshed through a 100-µm strainer. Percoll gradient centrifugation (37.5%) was used for further leukocyte purification from lung and small intestine cell suspensions. Afterward, erythrocytes in lung and bone marrow preparations were lysed with ACK lysis buffer. Bronchoalveolar lavage was performed by flushing the lungs with 500 µl PBS via a tracheal cannula.

Flow cytometry and cell sorting. To identify ILCs, isolated leukocytes were stained by using fluorochrome-coupled antibodies against CD45, Thy1.2, CD4, and a combination of lineage markers (Lin), including CD3, CD4, CD8, CD11b, CD11c, CD19, CD49b, TCR-β, TCR-γ, NK1.1, GR-1, and Ter119. For further characterization of ILC surface maker expression, antibodies against CD25, IL-7Rα (CD127), IL-33R (T1/ST2), ICOS, cKit, and Sca-1 were used. For characterization of macrophages and eosinophils, antibodies against CD11b, Ly6G, Ly6C, SiglecF, and CD11c were used. For cell culture experiments and real-time PCR, ILCs were sorted by flow cytometry based on the expression of Thy1.2 in the absence of all lineage markers. CD4^{+} T cells were sorted as CD4^{+}Thy1.2^{+}Lin^{+} cells, eosinophils were sorted as CD11b^{+}Ly6G^{-}SiglecF^{+}CD11c^{-}, and macrophages as Ly6G^{-}SiglecF^{-}CD11b^{+}F4/80^{hi}Ly6C^{lo}. Sorting purity was typically >95%. Cultured ILCs were stained with fluorochrome-coupled Annexin V in Annexin V–binding buffer according to the manufacturer's instruction (BioLegend), and dead cells were stained by addition of 7AAD (BioLegend). For intracellular cytokine staining, isolated leukocytes were restimulated with 0.5 µg/ml phorbol 12,13-dibutyrate and 0.5 µg/ml ionomycin in the presence of 1 µg/ml brefeldin A for 2.5 h, fixed with 3.8% formalin, permeabilized with 0.1% IGEPAL CA-630 (Sigma-Aldrich), and stained with combinations of fluorochrome-coupled antibodies against IL-4, IL-5, IL-13, IL-17A, and IFN-γ. Intranuclear staining, using an antibody against Ki67, GATA3 (clone L50-823), and ROR-γt (clone B2D) was performed with the Transcription Factor Staining Buffer Set (eBioscience) according to the manufacturer's instruction. All samples were acquired on a LSRII flow cytometer (BD) and analyzed with FlowJo software (Tree Star).

EdU incorporation assay. EdU (1 mg per mouse) was injected i.v. 2 h before sacrificing the mice. Incorporation of EdU was assessed by using the Click-iT EdU Cell Proliferation Assay (Invitrogen) according to the manufacturer's instruction.

ILC culture. ILCs sorted by flow cytometry were cultured in IMDM supplemented with 5% fetal calf serum, 2 mM L-glutamine, 50 nM β-

mercapto-ethanol, 100 U/liter penicillin, and 100 mg/ml streptomycin at a concentration of 2×10^5 per ml with or without 50 ng/ml IL-9 (R&D Systems) for 2 d.

Cytokine measurements. For cytokine measurements from lung homogenates, lungs were finely minced, supplemented with proteinase inhibitor (Complete; Roche) in 50 µl PBS, and spun over a 40-µm strainer, and the cell-free supernatant was collected. Cytokine concentrations in lung supernatants and in ILC culture supernatants were measured by using the bead-based cytokine detection assays FlowCytomix (eBioscience) or Cytometric Bead Array (BD) according to the manufacturers' instructions. Amphiregulin protein content of lung supernatants and ILC culture supernatants was measured by ELISA according to the manufacturer's instruction (R&D Systems).

Histology. After excision of the lungs, the left upper lobe was perfused with 500 µl neutral-buffered formalin (10%) via the main bronchus. The tissue was then fixed overnight in neutral-buffered formalin, washed in 75% ethanol, and embedded in paraffin. Lung sections were stained with Masson's trichrome, Prussian blue, and periodic acid–Schiff according to standard laboratory procedures. Immunohistochemistry was performed by using antibodies against mast cell tryptase (clone EPR847; Abcam) or cleaved caspase-3 (clone Asp175; Cell Signaling Technology), followed by development of the tissue sections with the ZytoChem Plus (AP) Polymer kit (Zytomed) according to the manufacturer's instruction. Slides were scanned with a VS120-SL slide scanner (Olympus). Images were analyzed with the OlyVIA image viewer (Olympus) and ImageJ software (National Institutes of Health). Emphysema-like damage was quantified by measuring the lung area affected by bullae formation with destruction of the regular tissue architecture and expressed as a percentage of total lung area of the section. Prussian blue–positive macrophages and mast cell tryptase–positive cells were counted manually in an area of at least 2.5 mm^2 and cleaved caspase-3–positive, nonepithelial, lymphoid cells were counted manually in an area of at least 10 mm^2 per lung section. Both were expressed as cell number per mm^2.

Lung function measurement. Baseline lung function parameters of conscious mice were obtained with a Buxco FinePointe System for noninvasive airway measurement (Buxco Research Systems) according to the manufacturer's instructions.

Real-time PCR. RNA from sorted ILCs and $CD4^+$ T cells was extracted by using the TRIzol Reagent (Life Technologies) and reversely transcribed with the Omniscript RT kit (QIAGEN) according to the manufacturers' instructions. TaqMan Gene Expression Assays in combination with the Universal PCR Master Mix and the ABI-Prism 7900 system (all Applied Biosystems) were used for quantification of the housekeeping gene (*Hprt1*) and the genes of interest. Target gene quantification was normalized to *Hprt1* gene expression.

Statistical analyses. The Student's *t* test was used for comparison between two groups. In case of three or more groups, one-way ANOVA was used, followed by a post hoc analysis with Bonferroni's test for multiple comparisons or Dunnett's test for comparison of all time points versus control.

We thank, Y. Li, H. Müller, and R. Mahmood for excellent technical assistance, R. Maizels for providing the L3 stage larvae to set up the *N. brasiliensis* life cycle, and the Division of Biological Services at the National Institute for Medical Research for breeding and maintenance of our mouse strains.

This work was supported by the Medical Research Council UK (grants U.117512792 and MC_UP_A253_1028), a Research Fellowship from the Deutsche Forschungsgemeinschaft (DFG) to J.-E. Turner (TU 316/1-1), and a DGF grant to U. Panzer (Klinische Forschergruppe 228 TP1, PA 754/7).

The authors have no competing financial interests.

Submitted: 10 January 2013
Accepted: 25 October 2013

REFERENCES

Allen, J.E., and R.M. Maizels. 2011. Diversity and dialogue in immunity to helminths. *Nat. Rev. Immunol.* 11:375–388. http://dx.doi.org/10.1038/nri2992

Angkasekwinai, P., S.H. Chang, M. Thapa, H. Watarai, and C. Dong. 2010. Regulation of IL-9 expression by IL-25 signaling. *Nat. Immunol.* 11:250–256. http://dx.doi.org/10.1038/ni.1846

Barlow, J.L., A. Bellosi, C.S. Hardman, L.F. Drynan, S.H. Wong, J.P. Cruickshank, and A.N. McKenzie. 2012. Innate IL-13-producing nuocytes arise during allergic lung inflammation and contribute to airways hyperreactivity. *J. Allergy Clin. Immunol.* 129:191–198. http://dx.doi.org/10.1016/j.jaci.2011.09.041

Bauer, A., A. Villunger, V. Labi, S.F. Fischer, A. Strasser, H. Wagner, R.M. Schmid, and G. Häcker. 2006. The NF-kappaB regulator Bcl-3 and the BH3-only proteins Bim and Puma control the death of activated T cells. *Proc. Natl. Acad. Sci. USA.* 103:10979–10984. http://dx.doi.org/10.1073/pnas.0603625103

Camberis, M., G. Le Gros, and J. Urban Jr. 2003. Animal model of *Nippostrongylus brasiliensis* and *Heligmosomoides polygyrus*. *Curr. Protoc. Immunol.* Chapter 19:Unit 19.12.

Chang, H.C., S. Sehra, R. Goswami, W. Yao, Q. Yu, G.L. Stritesky, R. Jabeen, C. McKinley, A.N. Ahyi, L. Han, et al. 2010. The transcription factor PU.1 is required for the development of IL-9-producing T cells and allergic inflammation. *Nat. Immunol.* 11:527–534. http://dx.doi.org/10.1038/ni.1867

Chang, Y.J., H.Y. Kim, L.A. Albacker, N. Baumgarth, A.N. McKenzie, D.E. Smith, R.H. Dekruyff, and D.T. Umetsu. 2011. Innate lymphoid cells mediate influenza-induced airway hyper-reactivity independently of adaptive immunity. *Nat. Immunol.* 12:631–638. http://dx.doi.org/10.1038/ni.2045

Chen, F., Z. Liu, W. Wu, C. Rozo, S. Bowdridge, A. Millman, N. Van Rooijen, J.F. Urban Jr., T.A. Wynn, and W.C. Gause. 2012. An essential role for TH2-type responses in limiting acute tissue damage during experimental helminth infection. *Nat. Med.* 18:260–266. http://dx.doi.org/10.1038/nm.2628

Cheng, G., M. Arima, K. Honda, H. Hirata, F. Eda, N. Yoshida, F. Fukushima, Y. Ishii, and T. Fukuda. 2002. Anti-interleukin-9 antibody treatment inhibits airway inflammation and hyperreactivity in mouse asthma model. *Am. J. Respir. Crit. Care Med.* 166:409–416. http://dx.doi.org/10.1164/rccm.2105079

Dardalhon, V., A. Awasthi, H. Kwon, G. Galileos, W. Gao, R.A. Sobel, M. Mitsdoerffer, T.B. Strom, W. Elyaman, I.C. Ho, et al. 2008. IL-4 inhibits TGF-beta-induced Foxp3+ T cells and, together with TGF-beta, generates IL-9+ IL-10+ Foxp3(-) effector T cells. *Nat. Immunol.* 9:1347–1355. http://dx.doi.org/10.1038/ni.1677

Deng, G., and E.R. Podack. 1993. Suppression of apoptosis in a cytotoxic T-cell line by interleukin 2-mediated gene transcription and deregulated expression of the protooncogene bcl-2. *Proc. Natl. Acad. Sci. USA.* 90:2189–2193. http://dx.doi.org/10.1073/pnas.90.6.2189

Elyaman, W., E.M. Bradshaw, C. Uyttenhove, V. Dardalhon, A. Awasthi, J. Imitola, E. Bettelli, M. Oukka, J. van Snick, J.C. Renauld, et al. 2009. IL-9 induces differentiation of TH17 cells and enhances function of FoxP3+ natural regulatory T cells. *Proc. Natl. Acad. Sci. USA.* 106:12885–12890. http://dx.doi.org/10.1073/pnas.0812530106

Fallon, P.G., P. Smith, E.J. Richardson, F.J. Jones, H.C. Faulkner, J. Van Snick, J.C. Renauld, R.K. Grencis, and D.W. Dunne. 2000. Expression of interleukin-9 leads to Th2 cytokine-dominated responses and fatal enteropathy in mice with chronic Schistosoma mansoni infections. *Infect. Immun.* 68:6005–6011. http://dx.doi.org/10.1128/IAI.68.10.6005-6011.2000

Fallon, P.G., S.J. Ballantyne, N.E. Mangan, J.L. Barlow, A. Dasvarma, D.R. Hewett, A. McIlgorm, H.E. Jolin, and A.N. McKenzie. 2006. Identification of an interleukin (IL)-25–dependent cell population that provides IL-4, IL-5, and IL-13 at the onset of helminth expulsion. *J. Exp. Med.* 203:1105–1116. http://dx.doi.org/10.1084/jem.20051615

Fontaine, R.H., O. Cases, V. Lelièvre, B. Mesplès, J.C. Renauld, G. Loron, V. Degos, P. Dournaud, O. Baud, and P. Gressens. 2008. IL-9/IL-9 receptor signaling selectively protects cortical neurons against developmental apoptosis. *Cell Death Differ.* 15:1542–1552. http://dx.doi.org/10.1038/cdd.2008.79

Fort, M.M., J. Cheung, D. Yen, J. Li, S.M. Zurawski, S. Lo, S. Menon, T. Clifford, B. Hunte, R. Lesley, et al. 2001. IL-25 induces IL-4, IL-5, and IL-13 and Th2-associated pathologies in vivo. *Immunity*. 15:985–995. http://dx.doi.org/10.1016/S1074-7613(01)00243-6

Godfraind, C., J. Louahed, H. Faulkner, A. Vink, G. Warnier, R. Grencis, and J.C. Renauld. 1998. Intraepithelial infiltration by mast cells with both connective tissue-type and mucosal-type characteristics in gut, trachea, and kidneys of IL-9 transgenic mice. *J. Immunol.* 160:3989–3996.

Goswami, R., and M.H. Kaplan. 2011. A brief history of IL-9. *J. Immunol.* 186:3283–3288. http://dx.doi.org/10.4049/jimmunol.1003049

Gounni, A.S., B. Gregory, E. Nutku, F. Aris, K. Latifa, E. Minshall, J. North, J. Tavernier, R. Levit, N. Nicolaides, et al. 2000. Interleukin-9 enhances interleukin-5 receptor expression, differentiation, and survival of human eosinophils. *Blood*. 96:2163–2171.

Harvie, M., M. Camberis, S.C. Tang, B. Delahunt, W. Paul, and G. Le Gros. 2010. The lung is an important site for priming CD4 T-cell-mediated protective immunity against gastrointestinal helminth parasites. *Infect. Immun.* 78:3753–3762. http://dx.doi.org/10.1128/IAI.00502-09

Heitmann, L., R. Rani, L. Dawson, C. Perkins, Y. Yang, J. Downey, C. Hölscher, and D.R. Herbert. 2012. TGF-β-responsive myeloid cells suppress type 2 immunity and emphysematous pathology after hookworm infection. *Am. J. Pathol.* 181:897–906. http://dx.doi.org/10.1016/j.ajpath.2012.05.032

Heredia, J.E., L. Mukundan, F.M. Chen, A.A. Mueller, R.C. Deo, R.M. Locksley, T.A. Rando, and A. Chawla. 2013. Type 2 innate signals stimulate fibro/adipogenic progenitors to facilitate muscle regeneration. *Cell*. 153:376–388. http://dx.doi.org/10.1016/j.cell.2013.02.053

Hoyler, T., C.S. Klose, A. Souabni, A. Turqueti-Neves, D. Pfeifer, E.L. Rawlins, D. Voehringer, M. Busslinger, and A. Diefenbach. 2012. The transcription factor GATA-3 controls cell fate and maintenance of type 2 innate lymphoid cells. *Immunity*. 37:634–648. http://dx.doi.org/10.1016/j.immuni.2012.06.020

Hültner, L., J. Moeller, E. Schmitt, G. Jäger, G. Reisbach, J. Ring, and P. Dörmer. 1989. Thiol-sensitive mast cell lines derived from mouse bone marrow respond to a mast cell growth-enhancing activity different from both IL-3 and IL-4. *J. Immunol.* 142:3440–3446.

Hültner, L., C. Druez, J. Moeller, C. Uyttenhove, E. Schmitt, E. Rüde, P. Dörmer, and J. Van Snick. 1990. Mast cell growth-enhancing activity (MEA) is structurally related and functionally identical to the novel mouse T cell growth factor P40/TCGFIII (interleukin 9). *Eur. J. Immunol.* 20:1413–1416. http://dx.doi.org/10.1002/eji.1830200632

Hurst, S.D., T. Muchamuel, D.M. Gorman, J.M. Gilbert, T. Clifford, S. Kwan, S. Menon, B. Seymour, C. Jackson, T.T. Kung, et al. 2002. New IL-17 family members promote Th1 or Th2 responses in the lung: in vivo function of the novel cytokine IL-25. *J. Immunol.* 169:443–453.

Jenkins, S.J., D. Ruckerl, P.C. Cook, L.H. Jones, F.D. Finkelman, N. van Rooijen, A.S. MacDonald, and J.E. Allen. 2011. Local macrophage proliferation, rather than recruitment from the blood, is a signature of TH2 inflammation. *Science*. 332:1284–1288. http://dx.doi.org/10.1126/science.1204351

Kearley, J., J.S. Erjefalt, C. Andersson, E. Benjamin, C.P. Jones, A. Robichaud, S. Pegorier, Y. Brewah, T.J. Burwell, L. Bjermer, et al. 2011. IL-9 governs allergen-induced mast cell numbers in the lung and chronic remodeling of the airways. *Am. J. Respir. Crit. Care Med.* 183:865–875. http://dx.doi.org/10.1164/rccm.200909-1462OC

Liang, H.E., R.L. Reinhardt, J.K. Bando, B.M. Sullivan, I.C. Ho, and R.M. Locksley. 2012. Divergent expression patterns of IL-4 and IL-13 define unique functions in allergic immunity. *Nat. Immunol.* 13:58–66. http://dx.doi.org/10.1038/ni.2182

Marsland, B.J., M. Kurrer, R. Reissmann, N.L. Harris, and M. Kopf. 2008. *Nippostrongylus brasiliensis* infection leads to the development of emphysema associated with the induction of alternatively activated macrophages. *Eur. J. Immunol.* 38:479–488. http://dx.doi.org/10.1002/eji.200737827

McMillan, S.J., B. Bishop, M.J. Townsend, A.N. McKenzie, and C.M. Lloyd. 2002. The absence of interleukin 9 does not affect the development of allergen-induced pulmonary inflammation nor airway hyperreactivity. *J. Exp. Med.* 195:51–57. http://dx.doi.org/10.1084/jem.20011732

Mjösberg, J.M., S. Trifari, N.K. Crellin, C.P. Peters, C.M. van Drunen, B. Piet, W.J. Fokkens, T. Cupedo, and H. Spits. 2011. Human IL-25- and IL-33-responsive type 2 innate lymphoid cells are defined by expression of CRTH2 and CD161. *Nat. Immunol.* 12:1055–1062. http://dx.doi.org/10.1038/ni.2104

Mjösberg, J., J. Bernink, K. Golebski, J.J. Karrich, C.P. Peters, B. Blom, A.A. te Velde, W.J. Fokkens, C.M. van Drunen, and H. Spits. 2012. The transcription factor GATA3 is essential for the function of human type 2 innate lymphoid cells. *Immunity*. 37:649–659. http://dx.doi.org/10.1016/j.immuni.2012.08.015

Mohrs, K., A.E. Wakil, N. Killeen, R.M. Locksley, and M. Mohrs. 2005. A two-step process for cytokine production revealed by IL-4 dual-reporter mice. *Immunity*. 23:419–429. http://dx.doi.org/10.1016/j.immuni.2005.09.006

Monticelli, L.A., G.F. Sonnenberg, M.C. Abt, T. Alenghat, C.G. Ziegler, T.A. Doering, J.M. Angelosanto, B.J. Laidlaw, C.Y. Yang, T. Sathaliyawala, et al. 2011. Innate lymphoid cells promote lung-tissue homeostasis after infection with influenza virus. *Nat. Immunol.* 12:1045–1054. http://dx.doi.org/10.1038/ni.2131

Moro, K., T. Yamada, M. Tanabe, T. Takeuchi, T. Ikawa, H. Kawamoto, J. Furusawa, M. Ohtani, H. Fujii, and S. Koyasu. 2010. Innate production of T(H)2 cytokines by adipose tissue-associated c-Kit(+)Sca-1(+) lymphoid cells. *Nature*. 463:540–544. http://dx.doi.org/10.1038/nature08636

Neill, D.R., S.H. Wong, A. Bellosi, R.J. Flynn, M. Daly, T.K. Langford, C. Bucks, C.M. Kane, P.G. Fallon, R. Pannell, et al. 2010. Nuocytes represent a new innate effector leukocyte that mediates type-2 immunity. *Nature*. 464:1367–1370. http://dx.doi.org/10.1038/nature08900

Parker, J.M., C.K. Oh, C. LaForce, S.D. Miller, D.S. Pearlman, C. Le, G.J. Robbie, W.I. White, B. White, and N.A. Molfino; MEDI-528 Clinical Trials Group. 2011. Safety profile and clinical activity of multiple subcutaneous doses of MEDI-528, a humanized anti-interleukin-9 monoclonal antibody, in two randomized phase 2a studies in subjects with asthma. *BMC Pulm. Med.* 11:14. http://dx.doi.org/10.1186/1471-2466-11-14

Price, A.E., H.E. Liang, B.M. Sullivan, R.L. Reinhardt, C.J. Eisley, D.J. Erle, and R.M. Locksley. 2010. Systemically dispersed innate IL-13-expressing cells in type 2 immunity. *Proc. Natl. Acad. Sci. USA*. 107:11489–11494. http://dx.doi.org/10.1073/pnas.1003988107

Rebollo, A., L. Dumoutier, J.C. Renauld, A. Zaballos, V. Ayllón, and C. Martínez-A. 2000. Bcl-3 expression promotes cell survival following interleukin-4 deprivation and is controlled by AP1 and AP1-like transcription factors. *Mol. Cell. Biol.* 20:3407–3416. http://dx.doi.org/10.1128/MCB.20.10.3407-3416.2000

Richard, M., J. Louahed, J.B. Demoulin, and J.C. Renauld. 1999. Interleukin-9 regulates NF-kappaB activity through BCL3 gene induction. *Blood*. 93:4318–4327.

Saenz, S.A., M.C. Siracusa, J.G. Perrigoue, S.P. Spencer, J.F. Urban Jr., J.E. Tocker, A.L. Budelsky, M.A. Kleinschek, R.A. Kastelein, T. Kambayashi, et al. 2010. IL25 elicits a multipotent progenitor cell population that promotes T(H)2 cytokine responses. *Nature*. 464:1362–1366. http://dx.doi.org/10.1038/nature08901

Schmitt, E., R. Van Brandwijk, J. Van Snick, B. Siebold, and E. Rüde. 1989. TCGF III/P40 is produced by naive murine CD4+ T cells but is not a general T cell growth factor. *Eur. J. Immunol.* 19:2167–2170. http://dx.doi.org/10.1002/eji.1830191130

Spits, H., and J.P. Di Santo. 2011. The expanding family of innate lymphoid cells: regulators and effectors of immunity and tissue remodeling. *Nat. Immunol.* 12:21–27. http://dx.doi.org/10.1038/ni.1962

Staudt, V., E. Bothur, M. Klein, K. Lingnau, S. Reuter, N. Grebe, B. Gerlitzki, M. Hoffmann, A. Ulges, C. Taube, et al. 2010. Interferon-regulatory factor 4 is essential for the developmental program of T helper 9 cells. *Immunity*. 33:192–202. http://dx.doi.org/10.1016/j.immuni.2010.07.014

Steenwinckel, V., J. Louahed, C. Orabona, F. Huaux, G. Warnier, A. McKenzie, D. Lison, R. Levitt, and J.C. Renauld. 2007. IL-13 mediates in vivo IL-9 activities on lung epithelial cells but not on hematopoietic cells. *J. Immunol.* 178:3244–3251.

Temann, U.A., P. Ray, and R.A. Flavell. 2002. Pulmonary overexpression of IL-9 induces Th2 cytokine expression, leading to immune pathology. *J. Clin. Invest.* 109:29–39.

Temann, U.A., Y. Laouar, E.E. Eynon, R. Homer, and R.A. Flavell. 2007. IL9 leads to airway inflammation by inducing IL13 expression in airway epithelial cells. *Int. Immunol.* 19:1–10.

Townsend, J.M., G.P. Fallon, J.D. Matthews, P. Smith, E.H. Jolin, and N.A. McKenzie. 2000. IL-9-deficient mice establish fundamental roles for IL-9 in pulmonary mastocytosis and goblet cell hyperplasia but not T cell development. *Immunity*. 13:573–583. http://dx.doi.org/10.1016/S1074-7613(00)00056-X

Uyttenhove, C., R.J. Simpson, and J.Van Snick. 1988. Functional and structural characterization of P40, a mouse glycoprotein with T-cell growth factor activity. *Proc. Natl. Acad. Sci. USA*. 85:6934–6938. http://dx.doi.org/10.1073/pnas.85.18.6934

Veldhoen, M., C. Uyttenhove, J. van Snick, H. Helmby, A. Westendorf, J. Buer, B. Martin, C. Wilhelm, and B. Stockinger. 2008. Transforming growth factor-beta 'reprograms' the differentiation of T helper 2 cells and promotes an interleukin 9-producing subset. *Nat. Immunol.* 9:1341–1346. http://dx.doi.org/10.1038/ni.1659

Voehringer, D., T.A. Reese, X. Huang, K. Shinkai, and R.M. Locksley. 2006. Type 2 immunity is controlled by IL-4/IL-13 expression in hematopoietic non-eosinophil cells of the innate immune system. *J. Exp. Med*. 203:1435–1446. http://dx.doi.org/10.1084/jem.20052448

von Freeden-Jeffry, U., N. Solvason, M. Howard, and R. Murray. 1997. The earliest T lineage-committed cells depend on IL-7 for Bcl-2 expression and normal cell cycle progression. *Immunity*. 7:147–154. http://dx.doi.org/10.1016/S1074-7613(00)80517-8

Wilhelm, C., K. Hirota, B. Stieglitz, J. Van Snick, M. Tolaini, K. Lahl, T. Sparwasser, H. Helmby, and B. Stockinger. 2011. An IL-9 fate reporter demonstrates the induction of an innate IL-9 response in lung inflammation. *Nat. Immunol.* 12:1071–1077. http://dx.doi.org/10.1038/ni.2133

Wilhelm, C., J.E. Turner, J.Van Snick, and B. Stockinger. 2012. The many lives of IL-9: a question of survival? *Nat. Immunol.* 13:637–641. http://dx.doi.org/10.1038/ni.2303

Wong, S.H., J.A. Walker, H.E. Jolin, L.F. Drynan, E. Hams, A. Camelo, J.L. Barlow, D.R. Neill, V. Panova, U. Koch, et al. 2012. Transcription factor RORα is critical for nuocyte development. *Nat. Immunol.* 13:229–236. http://dx.doi.org/10.1038/ni.2208

Yasuda, K., T. Muto, T. Kawagoe, M. Matsumoto, Y. Sasaki, K. Matsushita, Y. Taki, S. Futatsugi-Yumikura, H. Tsutsui, K.J. Ishii, et al. 2012. Contribution of IL-33-activated type II innate lymphoid cells to pulmonary eosinophilia in intestinal nematode-infected mice. *Proc. Natl. Acad. Sci. USA*. 109:3451–3456. http://dx.doi.org/10.1073/pnas.1201042109

Zaiss, D.M., L. Yang, P.R. Shah, J.J. Kobie, J.F. Urban, and T.R. Mosmann. 2006. Amphiregulin, a TH2 cytokine enhancing resistance to nematodes. *Science*. 314:1746. http://dx.doi.org/10.1126/science.1133715